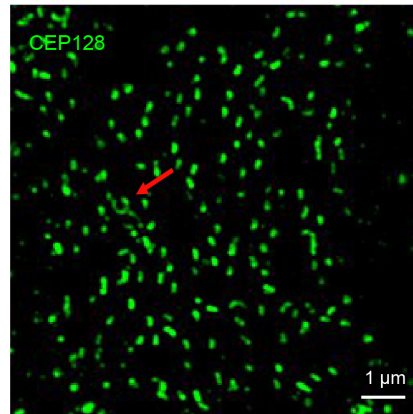
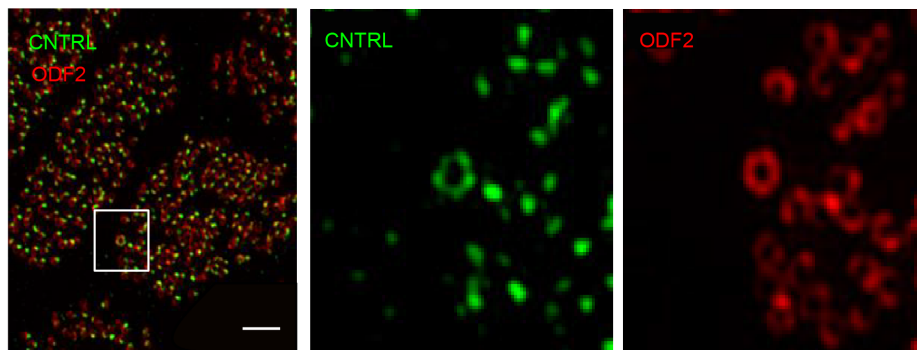


## Supplementary figures

A



B



**Figure S1. ODF2 and CEP128 localization at hybrid cilium in human airway multiciliated cells. Related to Figure 1.**

(A) 2D projection micrograph of 3DSIM volume of human airway multiciliated cell labeled with anti-CEP128 antibody. Arrows indicate hybrid cilia with ring-like distribution of basal feet labeled by anti-CEP128 antibodies. Scale bar represents 1  $\mu\text{m}$ . (B) Left: 2D projection micrograph of 3DSIM volume of human airway multiciliated cells. Right: high-magnification view of the boxed area with individual channels (middle and right), labeled with anti-CNTRL (green) and anti-ODF2 (red) antibodies, showing a ring-like distribution of basal feet labeled with CNTRL. Scale bar represents 2  $\mu\text{m}$ .

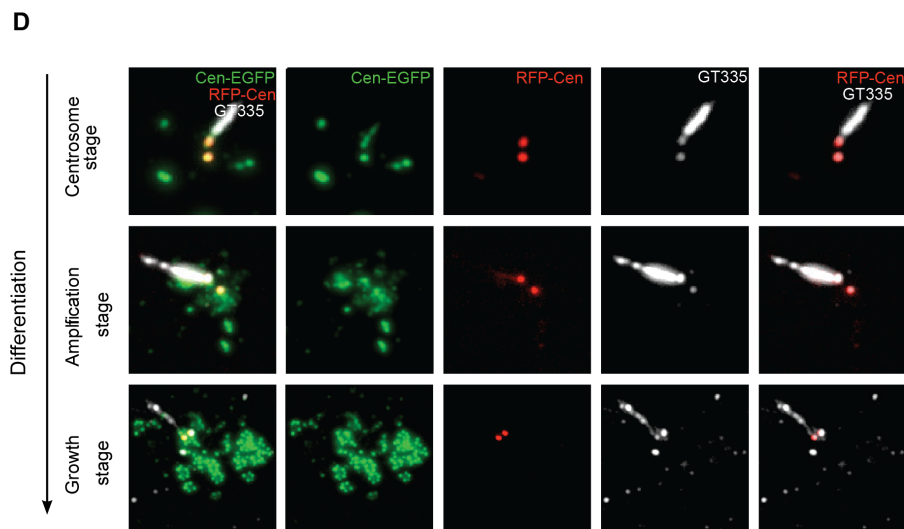
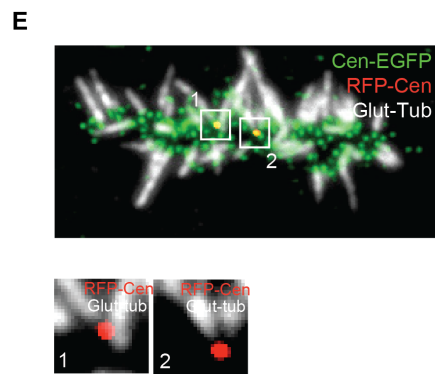
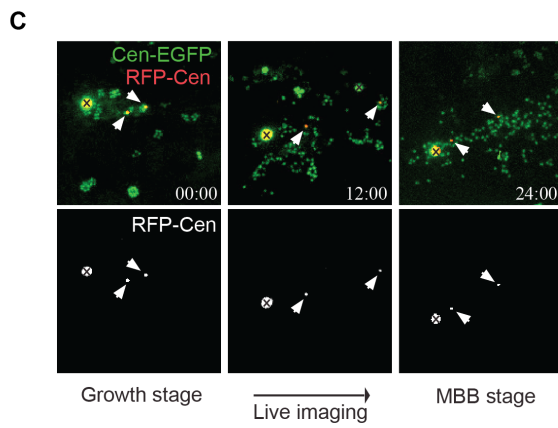
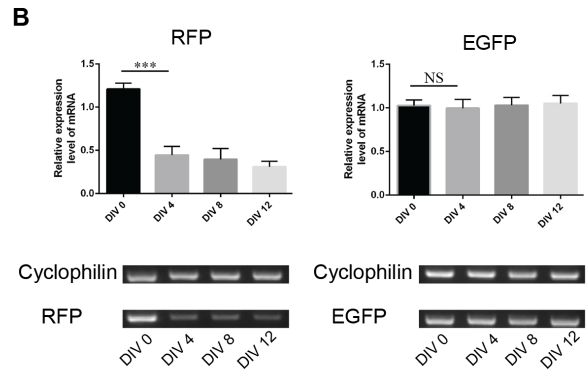
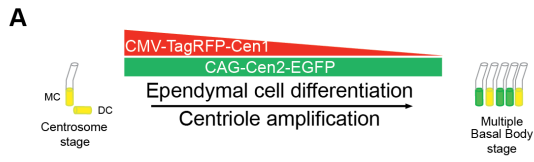


**Figure S2. Maternal centriole is retained in the basal body patch in ependymal multiciliated cells. Related to Figure 4 and the “MTEC and ependymal cell experiments” part of the STAR METHODS.**

(A) Cartoon depiction of the pulse-chase experiment using TagRFP-Cen1 ectopic expression in Cen2-EFGP transgenic primary cultured ependymal cells. (B) Semi-quantitative RT-PCR experiments show that TagRFP-Cen1 expression drops between DIV0 and DIV4 allowing the specific tagging of centrosomal centrioles with TagRFP in some cells. (C) Live imaging of TagRFP-Cen1 centrosomal centrioles during centriole amplification in primary cultured ependymal progenitors from Cen2-EFGP mice. Newly formed EGFP+ procentrioles are growing from deuterosomes and RFP+ centrosomal centrioles (00:00) before disengaging from their growing platforms (12:00) and gathering all together in the basal body patch (24:00). Arrowheads point to RFP+ centrosomal centrioles. A «x» sign marks centrin aggregates. (D) 2D projection micrographs from immunofluorescence experiments of ependymal progenitor cells expressing TagRFP-Cen1, Cen2-EGFP and labelled with anti-Glutamylated antibodies (GT335) to label cilia. Note that the different temporal expression of the markers allows a selective labelling of GT335+ centrosomal centrioles with TagRFP-Cen1 in differentiating ependymal cells. (E) 2D projection micrograph from immunostaining experiment of primary cultured ependymal multiciliated cell expressing TagRFP-Cen1, Cen2-EGFP and labelled with glutamylated-tubulin (GT335) which suggests that RFP+ centrosomal centrioles are retained in the basal body patch and can grow cilia.

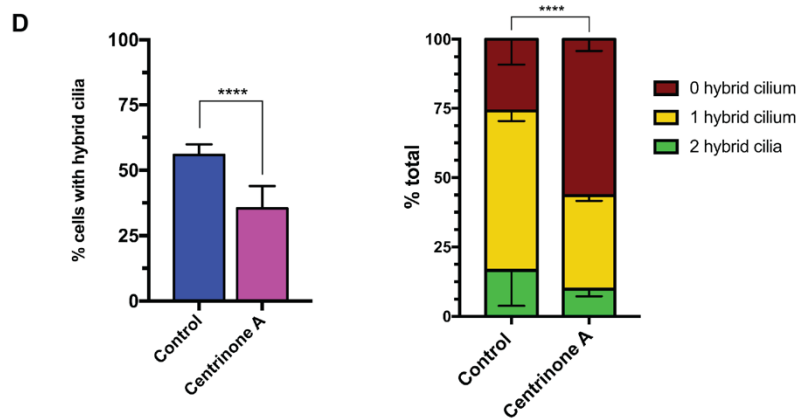
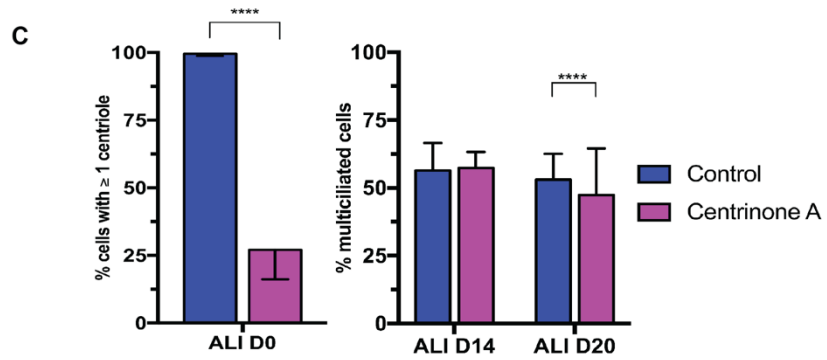
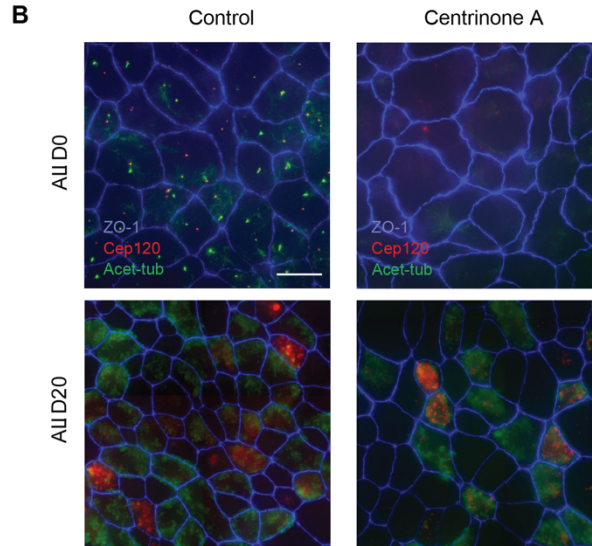
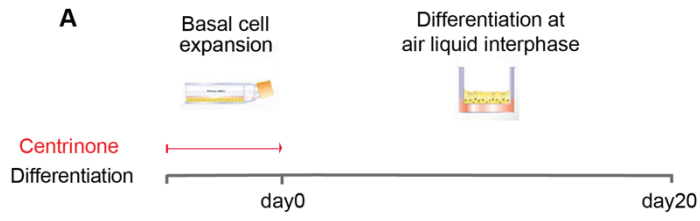


**Figure S3. Centrinone treatment blocks centriole duplication but does not affect multiciliogenesis. Related to Figure 4.**

(A) Cartoon representation of centrinone A treatment in mouse tracheal multiciliated cells.

(B) 3DSIM volume maximum intensity projections of mouse tracheal multiciliated cells at ALI D0 (left) and ALI D20 (right), treated with DMSO control or centrinone A and labeled with anti-acetylated tubulin (green), anti-CEP120 (red) and anti-ZO-1 (blue) antibodies. Scale bars represent 10  $\mu\text{m}$ .

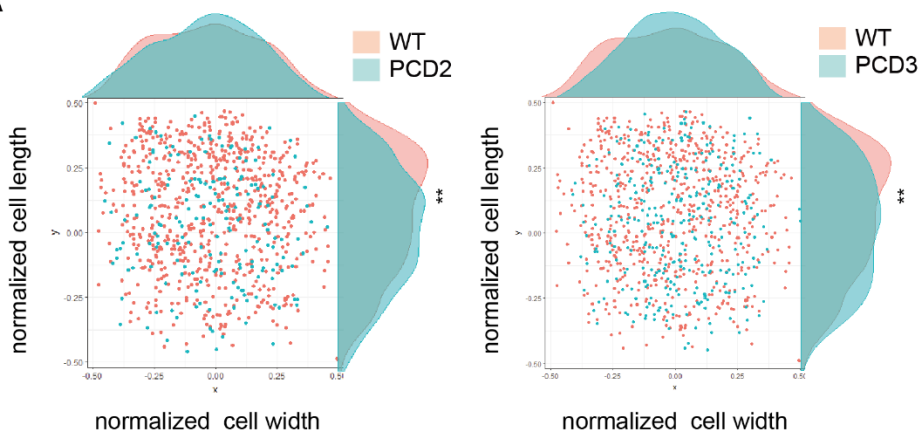
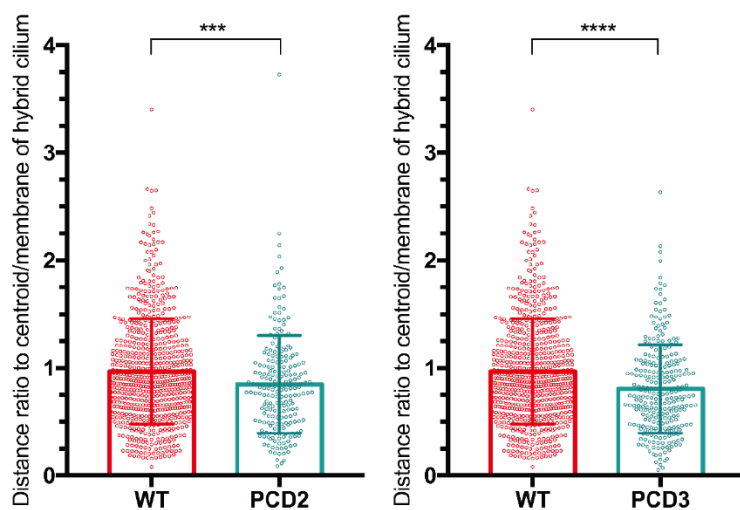
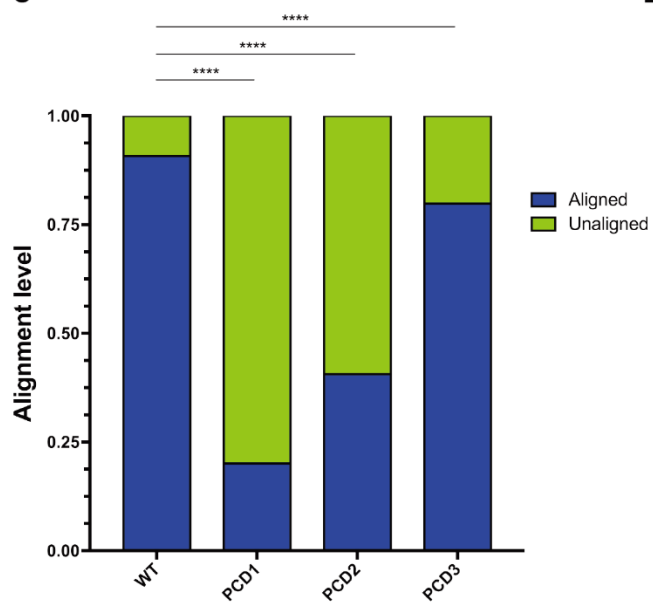
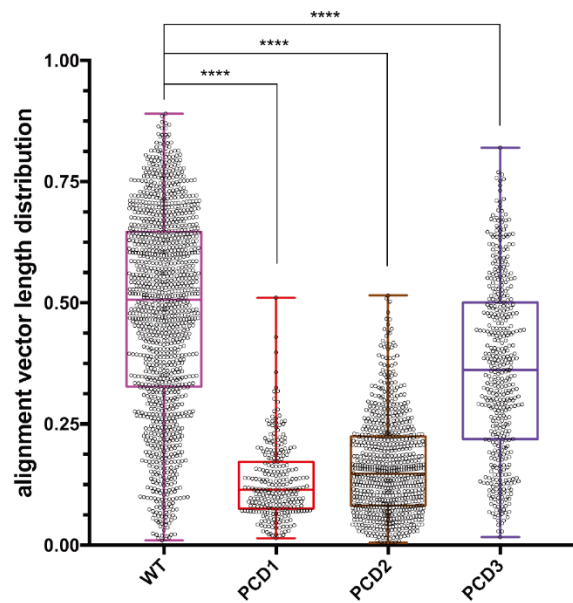
(C) Bar graph showing percentage of cells with more than one centriole at ALI D0 (left) and percentage of multiciliated cells at ALI D14 and D20 (right) in DMSO control

(blue) or centrinone A treated during basal cells expansion (pink);  $n > 6000$ . Data are represented as mean  $\pm$  SD. Statistical analysis was done using Cochran-Mantel-Haenszel test.

(D) Left and middle: Bar graphs representing percentage of cells with hybrid cilium in DMSO control (blue) and centrinone A-treated (pink) cells treated during basal cell expansion, with (middle) or without normalization to control condition;  $n > 800$ . Statistical analysis was done using Cochran-

Mantel-Haenszel test. Right: Bar graph representing percentage of cells with none (red), one (yellow) or two (green) hybrid cilia in ALI D20 mouse tracheal multiciliated cells treated with DMSO control (left) or centrinone A (right);  $n > 800$ . Data are represented as mean  $\pm$  SD.

Statistical analysis was done using chi-square test.

**A****B****C****D**



**Figure S4. Hybrid cilium position is biased toward the beating direction. Related to Figure 6.**

(A) Scatterplot showing the cumulative distribution of hybrid cilia along normalized cell width and cell length in human airway multiciliated cells from healthy individuals or PCD patients with immotile cilia caused by loss-of-function mutations in DNAH11 (PCD2 p.[(Cys4286\*)]; [(Ile4122Ser)]) and DNAH5 (PCD3 p.[(Phe634Serfs\*2)]) and, indicating a positional bias toward the direction of ciliary beating. Each dot represents a hybrid cilium in a cell; Healthy n=694, PCD2= 188, PCD3= 322. Statistical analysis was done using t test. \*\*, p< 0.01. (B) Scatterplot-bar graphs showing distribution of ratio of hybrid cilium-cell centroid distance to hybrid cilium-cell membrane shortest distance of human airway multiciliated cells from healthy individuals (red, n=686) or PCD patients. with immotile cilia caused by loss-of-function mutations in DNAH5 (blue, PCD2 n=222, PCD3 n=275). Each dot represents the position of a hybrid cilium in a cell. Data are represented as mean  $\pm$  SD. Statistical analysis was done using Welch's t-test. \*\*\* p<0.001, \*\*\*\* p<0.0001. (C) Stacked column graph showing the percentage of aligned (blue) and unaligned (green) cells over total cell population of WT (n=1267), PCD1 (n=274), PCD2 (n=763), and PCD3 (n=451). Statistical test was conducted using Fisher's exact test. \*\*\*\* p<0.0001. (D) Boxplot representing alignment vector length distribution of WT (n=1273), PCD1 (n=277), PCD2 (n=792), and PCD3 (n=453). Data are represented as mean  $\pm$  SD. Statistical test was conducted using one-way ANOVA and Tukey's multiple comparison test. \*\*\*\* p<0.0001.